European Radiology (2021) 31:4794–4803
https://doi.org/10.1007/s00330-020-07457-6

HEPATOBILIARY-PANCREAS

# Evaluation of LI-RADS 3 category by magnetic resonance in US-detected nodules ≤ 2 cm in cirrhotic patients

Anna Darnell[1] · Jordi Rimola[1] · Ernest Belmonte[1] · Enric Ripoll[1] · Ángeles Garcia-Criado[1] · Carla Caparroz[1] · Álvaro Díaz-González[2] · Ramón Vilana[1,2] · María Reig[2,3] · Carmen Ayuso[1,3] · Jordi Bruix[2,3] · Alejandro Forner[2,3]

Received: 5 May 2020 / Revised: 15 September 2020 / Accepted: 3 November 2020 / Published online: 6 January 2021
© European Society of Radiology 2021

## Abstract

**Objectives** Liver Imaging Reporting and Data System (LI-RADS) for hepatocellular carcinoma (HCC) diagnosis in high-risk patients is a dynamic system, which was lastly updated in 2018. We aimed to evaluate the accuracy for HCC diagnosis of LI-RADS v2018 with magnetic resonance imaging (MRI) with extracellular contrast for solitary nodules ≤ 20 mm detected during ultrasound (US) surveillance in cirrhotic patients, with particular interest in those observations categorized as LI-RADS 3.

**Methods** Between November 2003 and February 2017, we included 262 consecutive cirrhotic patients with a newly US-detected solitary ≤ 20-mm nodule. A LI-RADS (LR) v2018 category was retrospectively assigned. The diagnostic accuracy for each LR category was described, and the main MRI findings associated with HCC diagnosis were analyzed.

**Results** Final diagnoses were as follows: 197 HCC (75.2%), 5 cholangiocarcinoma (1.9%), 2 metastasis (0.8%), and 58 benign lesions (22.1%); 0/15 (0%) LR-1, 6/26 (23.1%) LR-2, 51/74 (68.9%) LR-3, 11/12 (91.7%) LR-4, 126/127 (99.2%) LR-5, and 3/8 (37.5%) LR-M were HCC. LR-5 category displayed a sensitivity and specificity of 64% (95% CI, 56.8–70.7) and 98.5% (95% CI, 91.7–100), respectively. Considering also LR-4 as diagnostic for HCC, the sensitivity slightly increased to 69.5% (95% CI, 62.6–75.9) with minor impact on specificity (96.2%; 95% CI, 89.3–99.6). Regarding LR-3 observations, 51 out of 74 were HCC, 2 were non-HCC malignancies, and 20 out of 21 LR-3 nodules > 15 mm (95.2%) were finally categorized as HCC.

**Conclusions** The high probability of HCC in US-detected LR-3 observations (68.9%) justifies triggering an active diagnostic work-up if intended to diagnose HCC at a very early stage.

**Key Points**

- *In cirrhotic patients with nodules ≤ 20 mm detected during US surveillance, 51 out of 74 (68.9%) of LR-3 nodules by MRI corresponded to an HCC.*
- *In LR-3 nodules, HCC diagnosis was closely related to baseline tumor size. All 5 nodules smaller than 1 cm were diagnosed as benign. Oppositely, 20 out of 21 LR-3 observations > 15 mm (95.2%) were diagnosed as HCC.*
- *The high probability of HCC in US-detected LR-3 observations justifies triggering an active diagnostic work-up if intended to diagnose HCC at a very early stage.*

**Keywords** Diagnosis · Ultrasonography · Hepatocellular carcinoma · Cirrhosis · Sensitivity and specificity

✉ Alejandro Forner
aforner@clinic.cat

[1] BCLC Group, Radiology Department, Hospital Clínic of Barcelona, IDIBAPS, University of Barcelona, Barcelona, Spain

[2] BCLC Group, Liver Unit, Hospital Clínic of Barcelona, Fundació Clínic per a la Recerca Biomédica (FCRB), IDIBAPS, University of Barcelona, Villarroel 170, Escala 11, 4a planta, 08036 Barcelona, Spain

[3] Centro de Investigación Biomédica en Red de Enfermedades Hepáticas y Digestivas (CIBERehd), Barcelona, Spain

**Abbreviations**

| | |
|---|---|
| AASLD | American Association for the Study of Liver Diseases |
| ACR | American College of Radiology |
| CT | Computed tomography |
| EASL | European Association for the Study of the Liver |
| FNB | Fine-needle biopsy |
| HCC | Hepatocellular carcinoma |
| iCCA | Intrahepatic cholangiocarcinoma |
| LI-RADS/LR | Liver Imaging Reporting and Data System |

| | |
|---|---|
| MRI | Magnetic resonance imaging |
| NAFLD | Non-alcoholic fatty liver disease |
| US | Ultrasonography |

## Introduction

Hepatocellular carcinoma (HCC) usually develops in patients with chronic liver disease, and in this population, HCC has been recognized as a leading cause of death [1]. The prolonged subclinical course of this cancer and the identification of a target population at risk of developing HCC provide the opportunity for early detection through the implementation of surveillance programs [2, 3]. HCC surveillance relies on ultrasonography (US), and the unequivocal diagnosis of a US-detected nodule within a cirrhotic liver represents a major clinical challenge.

Aimed to develop a system for standardizing the terminology, technique, interpretation, reporting, and data collection of liver imaging in patients at risk of developing HCC, the American College of Radiology (ACR) developed the Liver Imaging Reporting and Data System (LI-RADS) [4]. The purpose of this system is to guide the diagnosis and management of liver observations identified by imaging techniques. LI-RADS classifies the full spectrum of liver lesions and pseudolesions in categories, ranging from benign to malignant/HCC lesions.

LI-RADS is a dynamic document originally released in 2011, which has been updated several times incorporating information regarding probabilities of benign, HCC, and other malignancies in each LI-RADS category. In that sense, the diagnostic performance of LI-RADS v2013 by MRI was evaluated in cirrhotic patients with a US-detected solitary nodule 20 mm or smaller. In those US-detected nodules, the LR-4 profile had a near-absolute specificity and, when combining both LR-4 and LR-5 as definitely HCC, the specificity was maintained with a significant increase in the sensitivity [5]. According to these results, an update of LI-RADS in 2014 (v2014) implemented the possibility of categorizing as LR-5us those LR-4 observations (10–19 mm with arterial phase hyperenhancement (APHE) and washout (WO) if visible on surveillance US), and this criterion was maintained until v2017. Another important finding of that study was that a relevant proportion of LR-3 observations (29 out of 42 patients, 69%) was finally diagnosed as HCC. Contrarily, in other studies, the proportion of HCC in LR-3 observations was lower, and most of these lesions remained stable or even decreased in category during follow-up, thus supporting the recommendation of imaging follow-up with no need for recalling an invasive work-up including percutaneous biopsy [6–9].

In 2018, the latest version of LI-RADS was released [10, 11]. The main changes compared to the previous version of 2017 were the simplification of the definition of threshold growth and the assignment of LR-5 category to observations between 10 and 19 mm displaying non-rim APHE and non-peripheral WO or threshold growth, regardless of their identification by US. With this latest update, LI-RADS is consistent with and fully integrated into the American Association for the Study of Liver Diseases (AASLD) clinical practice guidance [3].

The aim of this study is to evaluate the diagnostic accuracy of each LI-RADS category by MRI according to LI-RADS v2018 in a cohort of patients with cirrhosis in whom a solitary nodule ≤ 20 mm was detected during screening US, with particular interest in identifying which features are associated with the HCC diagnosis in nodules categorized as LR-3.

## Materials and methods

This study was approved by the institutional ethics committee for clinical research of our center, and the need to obtain consent for analysis of the data was waived. The inclusion was initiated in November 2003, and this assessment includes the patients recruited until February 2017 in order to ensure enough follow-up of patients with non-malignant diagnosis. Patients were Child-Pugh A-B with no history of HCC in whom a new solitary, well-defined, solid nodule between 5 and 20 mm was detected by screening ultrasound (US). Upon initial detection of hepatic nodule at screening US, patients were examined by dynamic MRI with extracellular contrast agent and finally submitted to ultrasound-guided biopsy. Pathology result was considered the gold standard, and biopsy was repeated if a conclusive diagnosis was not achieved. Since non-invasive criteria by MRI have been externally validated [12–14] and adopted as criteria for HCC diagnosis, we considered, after 2007, also the specific vascular profile (APHE and WO) by MRI as gold standard for HCC diagnosis, and if this was not present, pathology confirmation was requested. Nodules with neither pathological confirmation nor specific vascular pattern by MRI were followed with US every 3 months and MRI every 6 months, and a new biopsy was performed in case of growth or appearance of hypervascularization during the follow-up.

### MR imaging

MRI examinations were performed using clinical 1.5-T systems (Symphony or Aera; Siemens Healthineers, or Signa; General Electric Healthcare) with a torso phased-array coil for signal detection. A standard clinical liver MRI protocol was used in all patients with axial unenhanced breath-hold T1-weighted gradient-echo in-phase and out-of-phase and T2-weighted half-Fourier single-shot turbo spin-echo or single-shot fast spin-echo sequences. Then, an axial multiphase dynamic study with a 3D breath-hold fat-suppressed

T1-weighted interpolated spoiled gradient-echo sequence with extracellular gadolinium, at the recommended dose and rate (gadodiamide 0.5 mmol/mL, dose of 0.1 mmol/kg and rate of 2 mL/s; gadobutrol 1 mmol/mL, dose of 0.1 mmol/kg and rate of 2 mL/s), was done. After pre-contrast imaging, bolus tracking technique was used to obtain arterial-phase images, approximately 20 s after contrast injection. Portal venous and delayed venous phase images were acquired 60 to 65 s and 100 to 110 s, respectively, thereafter. Finally, a post-contrast axial 2D breath-hold fat-suppressed T1-weighted gradient-echo sequence was performed. Subtraction of the pre-contrast images from the arterial-phase images was performed. MRI with liver-specific contrast agent was not included in the analysis.

### Image interpretation

The first MRI obtained within 1 month after US nodule detection was read by one of three radiologists with more than 10 years of experience in imaging of the liver (A.D., J.R., and C.A.).

The analysis considers only the target lesion initially detected by screening US. The following items obtained by MRI were separately evaluated for each target lesion and prospectively registered in a case report form by J.R. and C.A.: size (in mm) and signal intensity in each sequence and in each phase of the dynamic study after intravenous contrast injection compared with that of the liver parenchyma and categorically classified as hyperintense, isointense, or hypointense at visual inspection. Occurrence of APHE (defined as non-rim-like enhancement in arterial phase unequivocally greater in whole or in part than the liver), and WO in venous phases, and presence of fat and "capsule" were specifically registered. Subtraction images were used for assessment of APHE in observations that were hyperintense on pre-contrast T1-weighted images.

A LI-RADS category according to LI-RADS v2108 [10] was retrospectively assigned by A.D. and C.C. by consensus. Only major features were used for category assignment of LI-RADS 3, 4, and 5 observations. Both radiologists were unaware of the final diagnosis of the lesion.

### Pathology diagnosis

Ultrasound-guided fine-needle aspiration was performed using a 20-gauge needle and/or core biopsy with an 18-gauge needle biopsy by an expert abdominal radiologist. Specimens were routinely processed and stained with hematoxylin–eosin. Diagnosis of HCC was made according to the criteria of the International Consensus Group for Hepatocellular Neoplasia [15].

### Statistical analysis

Comparison of patients with HCC and patients with non-HCC nodules was done by using Student's $t$ test, ANOVA, or the Mann–Whitney test for continuous variables and the chi-square test or Fisher's exact test for categorical variables. A $p$ value of less than 0.05 was considered significant. The diagnostic accuracy for each LI-RADS v2018 category was described by sensitivity, specificity, and positive/negative predictive values and was expressed with their 95% confident interval and compared with the accuracy of current European Association for the Study of the Liver (EASL) criteria. Calculations were done with the Stata package version 14 (StataCorp, 1985–2015).

## Results

Three hundred and fifteen cirrhotic patients with a single nodule equal or smaller than 20 mm detected by surveillance US were included. Fifty-one target nodules were not detected by MRI, and in two patients, the MRI was not technically adequate for a reliable evaluation: forty-two corresponded to benign lesions and the remaining eleven were finally diagnosed as HCC. Accordingly, LI-RADS v2018 categories were determined in the 262 target nodules identified in the first MRI after US detection (83.2% of the whole cohort). The final diagnosis of the 262 patients were as follows: 197 HCC (75.2%), 5 intrahepatic cholangiocarcinoma (iCCA) (1.9%), 2 metastases of a poorly differentiated neuroendocrine tumor and a colorectal adenocarcinoma (0.8%), and 58 benign lesions (22.1%) that were followed for a median of 16 months (interquartile range, 11.6–24.2) to assure the absence of malignancy (Fig. 1). Biopsy was done in 209 out of 262 nodules (79.8%), and the final diagnosis was pathologically confirmed in 196 nodules (74.8%): in 153 out of 197 HCC nodules, in 36 out of 58 benign lesions, and in all non-HCC malignant lesions. The main patients' characteristics are described in supplementary Table 1.

### LI-RADS v2018 categories

The LI-RADS v2018 categories and final diagnosis are summarized in Tables 1 and 2. Fifteen nodules were categorized as LR-1 (5.7%), 26 as LR-2 (9.9%), 74 as LR-3 (28.2%), 12 as LR-4 (4.6%), 127 as LR-5 (48.5%), and 8 as LR-M (3%).

All nodules categorized as LR-1 were confirmed as benign conditions. Six out of 26 LR-2 (23.1%) and 51 out of 74 LR-3 (68.9%) nodules were finally diagnosed as HCC. On the other hand, eleven out of 12 LR-4 (91.7%) and 126 out of 127 LR-5 (99.2%) nodules were finally diagnosed as HCC. The two false-positive diagnoses in LR-4 and LR-5 categories were

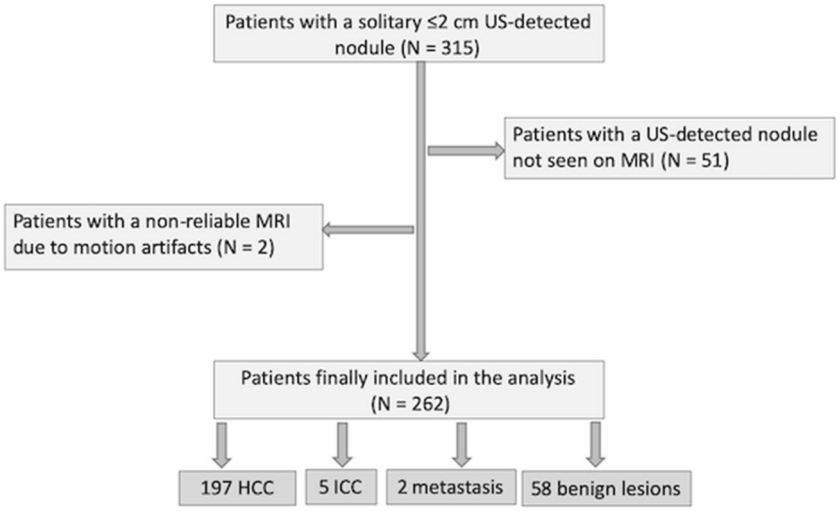


**Fig. 1** Flow chart of patients included in the analysis

an 18-mm poorly differentiated metastasis of a neuroendocrine tumor categorized as LR-5 and an arterial-hyperenhancing 20-mm nodule in an alcohol-related cirrhotic patient with a biopsy negative for malignancy, which disappeared during the work-up and did not reappear during more than 4 years of follow-up. It was classified as LR-4, and the final diagnosis was considered a regenerative nodule.

The eight nodules categorized as LR-M were 4 iCCA nodules of 14 mm, 20 mm, 20 mm, and 36 mm; 3 HCC nodules of 23 mm, 20 mm, and 15 mm; and a 15-mm nodule in a non-alcoholic fatty liver disease (NAFLD)-cirrhotic patient with two consecutive biopsies negative for malignancy, which disappeared during the work-up and did not reappear after more than 5 years of follow-up, categorized as regenerative nodule.

The diagnostic accuracies according to LI-RADS v2018 definitions are summarized in Table 3.

Since our study includes patients recruited during a long time period, in which the imaging acquisition has evolved, we separately analyzed those patients included from 2010 and results are summarized in supplementary Table 2. The distribution of LI-RADS categories and the probability of HCC were very similar to the whole cohort. Also, we evaluated the LI-RADS categories in only those patients with final diagnosis confirmed by pathology ($n$ = 196) (supplemental Table 3). In addition, tumor size was correlated with LI-RADS categories: Only 3 out of 15 LR-1 (20%) but 69 out of 127 LR-5 (54.4%) nodules were > 15 mm (supplementary Table 4).

## LI-RADS 2 category

Twenty-six nodules (9.9%) were categorized as LR-2. Six out of the 26 LR-2 nodules were finally diagnosed as HCC (23.1%) and the remaining 20 as benign nodules after a median follow-up of 12.3 months (IQR, 7–21). Five HCC nodules were diagnosed by histology, and median time from MRI to final HCC diagnosis was 4.5 months (IQR, 1.2–12 months). As seen in Table 4, the 6 LR-2 nodules finally diagnosed as

**Table 1** LI-RADS v2018 category of the 262 target lesions identified in the baseline MRI

| LI-RADS category | Final diagnosis | | | |
|---|---|---|---|---|
| | Total | HCC | Non-HCC malignant lesions | Benign lesions |
| LR-1 | 15 | 0 (0) | 0 (0) | 15 (100) |
| LR-2 | 26 | 6 (23.1) | 0 (0) | 20 (76.9) |
| LR-3 | 74 | 51 (68.9) | 2* (2.7) | 21 (28.4) |
| LR-4 | 12 | 11 (91.7) | 0 (0) | 1 (8.3) |
| LR-5 | 127 | 126 (99.2) | 1[#] (0.8) | 0 (0) |
| LR-M | 8 | 3 (37.5) | 4[$] (50) | 1 (12.5) |

The LI-RADS categories are correlated with final diagnosis. The percentage within each LI-RADS category is presented in the parentheses

*One intrahepatic cholangiocarcinoma of 14 mm and a 15-mm colorectal adenocarcinoma metastasis

[#] An 18-mm metastasis of a poorly differentiated neuroendocrine tumor

[$] Four intrahepatic cholangiocarcinoma 14 mm, 20 mm, 20 mm, and 36 mm

**Table 2** Categorization of the nodules considering major features (nodule size and presence of arterial phase hyperenhancement, washout and capsule)

| Arterial phase hyperenhancement (APHE) | | No-APHE | | Non-peripheral APHE | | |
|---|---|---|---|---|---|---|
| Observation size (mm) | | <20 | ≥ 20 | <10 | 10-19 | ≥ 20 |
| Count additional major features:<br>- Enhancing "capsule"<br>- Non-peripheral "washout"<br>- Threshold growth | None | 16 (10/6[#]) | 2 (1/1) | 5 (0/5) | 49 (38/11[$]) | 5 (4/1) |
| | One | 2 (2/0) | 1 (1/0) | 4 (4/0) | 1 (1/0)<br>56 (56/0) | 7 (7/0) |
| | ≥ Two | 0 (0/0) | 0 (0/0) | 1 (1/0) | 49 (48/1*) | 15 (15/0) |

LR-3

LR-4

LR-5

The number of nodules in each box and HCC vs. non-HCC is presented in the parentheses. Values in italics indicate LR-3, values in bold indicate LR-4, and values in bold–italics indicate LR-5

*An 18-mm nodule corresponding to a metastasis of a poorly differentiated neuroendocrine tumor

[#] This category includes a 15-mm colorectal adenocarcinoma metastasis

[$] This category included a 14-mm intrahepatic cholangiocarcinoma

HCC did not show any difference compared to those finally classified as benign.

## LI-RADS 3 category

The main patients' characteristics are described in supplementary Table 2, and the main MRI findings are summarized in Table 5. Seventy-four nodules (28.2%) were categorized as LR-3. Fifty-one out of the 74 (68.9%) were finally diagnosed as HCC (Fig. 2), two as non-HCC malignant lesions (one 14-mm iCCA and a 15-mm colorectal adenocarcinoma metastasis) and the remaining 21 as benign nodules after a median imaging follow-up of 17 months (IQR, 12–27.3). Forty-nine out of 51 HCC nodules were confirmed histologically and the remaining by non-invasive diagnosis criteria during the diagnostic work-up. The median time from MRI to final HCC diagnosis was 1.4 months (IQR, 0.6–6.2 months). HCC diagnosis was closely related to baseline tumor size: All 5 nodules smaller than 10 mm were diagnosed as benign. Oppositely, 31 out of 48 nodules 11–15 mm (64%) and 20 out of 21 LR-3 nodules > 15 mm (95.2%) were diagnosed as HCC. The nodule size was statistically associated with final HCC diagnosis ($p < 0.001$). The only LR-3 nodule > 15 mm without diagnosis of HCC was a 56-year-old woman with NAFLD-related cirrhosis in whom a 15-mm iso-hypoechoic nodule was detected on US. The MRI showed a 20-mm nodule hyperintense in T1-weighted images and hypointense in T2-weighted images, not identified in dynamic studies. A biopsy was indicated but was not feasible due to lack of an adequate percutaneous access. The nodule remained stable during more than 2 years and was categorized as benign.

**Table 3** Summary of the diagnostic accuracies for confident HCC diagnosis in nodules detected during US surveillance in patients with cirrhosis

| | Number of nodules | | | | Diagnostic performance, % (95% CI) | | | |
|---|---|---|---|---|---|---|---|---|
| | TP | FN | FP | TN | Sensitivity | Specificity | PPV | NPV |
| LR-5 | 126 | 71 | 1 | 64 | 64 (56.8–70.7) | 98.5 (91.7–100) | 99.2 (95.7–100) | 47.4 (38.8–56.2) |
| LR-4 + LR-5 | 137 | 60 | 2 | 63 | 69.5 (62.6–75.9) | 96.2 (89.3–99.6) | 98.6 (94.9–99.8) | 51.2 (42.1–60.3) |
| EASL criteria* | 124[#] | 73 | 1 | 65 | 62.9 (55.8–69.7) | 98.5 (91.7–100) | 99.2 (95.6–100) | 46.7 (38.2–55.4) |

*TP* true positive, *FN* false negative, *FP* false positive, *TN* true negative, *PPV* positive predictive value, *NPV* negative predictive value

*Nodules > 10 mm displaying the specific vascular pattern characterized as contrast uptake during arterial phase followed by contrast washout during the venous phases [2]

[#] A total of two observations not meeting EASL criteria but categorized as LR-5 were finally diagnosed as HCC: They corresponded to two lesions of 20 mm that displayed non-rim APHE and "capsule," without WO

**Table 4** MRI features of lesions categorized as LR-2

| LI-RADS 2 | All nodules ($n$ = 26) | HCC ($n$ = 6) | Non-HCC ($n$ = 20) | $p$ value |
|---|---|---|---|---|
| Size by MRI (median [range], in mm) | 13 [7–22] | 12 [9–18] | 13 [7–20] | 0.89 |
| < 10 mm, $n$ (%) | 7 (8.1) | 2 (2) | 5 (20.8) | |
| 10–15 mm, $n$ (%) | 14 (60.8) | 3 (56) | 11 (70.8) | |
| 16–20 mm, $n$ (%) | 5 (28.4) | 1 (38) | 4 (8.3) | |
| T1-weighted imaging, $n$ (%) | | | | |
| Not seen | 5 (19.2) | 3 (50) | 2 (10) | 0.37 |
| Isointense | 6 (23.1) | 1 (16.7) | 5 (25) | |
| Hypointense | 2 (7.7) | 0 (0) | 2 (10) | |
| Hyperintense | 13 (50) | 2 (33.3) | 11 (55) | |
| T2-weighted imaging, $n$ (%) | | | | |
| Not seen | 10 (32.4) | 3 (50) | 7 (35) | 0.32 |
| Isointense | 4 (21.6) | 1 (16.7) | 3 (15) | |
| Hypointense | 9 (34.6) | 2 (33.3) | 7 (35) | |
| Hyperintense | 3 (11.5) | 0 (0) | 3 (15) | |
| Arterial phase, $n$ (%) | | | | |
| Not seen | 8 (30.7) | 2 (33.3) | 6 (30) | 0.94 |
| Isointense | 11 (42.3) | 2 (33.3) | 9 (45) | |
| Hypointense | 2 (7.7) | 1 (16.7) | 1 (5) | |
| Hyperintense | 5 (19.2) | 1 (16.7) | 4 (20) | |
| Portal venous phase, $n$ (%) | | | | |
| Not seen | 7 (26.9) | 1 (16.7) | 6 (30) | 0.82 |
| Isointense | 10 (38.5) | 2 (33.3) | 8 (40) | |
| Hypointense | 8 (30.8) | 3 (50) | 5 (25) | |
| Hyperintense | 1 (3.8) | 0 (0) | 1 (5) | |
| Delayed venous phase, $n$ (%) | | | | |
| Not seen | 6 (23.1) | 1 (16.7) | 5 (25) | 0.87 |
| Isointense | 9 (34.6) | 2 (33.3) | 7 (35) | |
| Hypointense | 10 (32.4) | 3 (50) | 7 (35) | |
| Hyperintense | 1 (3.8) | 0 (0) | 1 (5) | |
| Non-peripheral washout (yes/no), $n$ (%) | 1/25 (3.9/96.1) | 1/5 (16.7/33.3) | 0/20 (0/100) | 1 |
| Enhancing capsule (yes/no), $n$ (%) | 0/26 (0/100) | 0/6 (0/100) | 0/20 (0/100) | 1 |
| Intralesional fat (yes/no), $n$ (%) | 6/20 (23.1/76.9) | 2/4 (33.3/66.7) | 4/16 (20/80) | 0.60 |

Other MRI findings, except more frequent hyperintense signal in T1-weighted imaging in HCC nodules, were not significantly different between HCC and non-HCC lesions (Table 5).

## Discussion

The main aim of the current study was to assess the diagnostic accuracy of each LI-RADS category by MRI according to LI-RADS v2018 and to evaluate the findings associated with HCC diagnosis in US-detected nodules ≤ 20 mm categorized as LR-3. In our cohort, 71.6% of LR-3 nodules corresponded to malignant lesions (51 HCC, 1 ICC, and 1 CRC metastasis). In addition, the median time from MRI to final HCC diagnosis in our series was 1.4 months (IQR, 0.6–6.2 months), which suggests that most of the LR-3 nodules were already HCC and not regenerative/dysplastic nodules that have evolved to HCC during the follow-up. This high proportion of malignancy in LR-3 category in US-detected nodules has been also reported by other authors [16, 17]. However, the high proportion of HCC in LR-3 category diverges from retrospective studies exploring the outcome of LR-3 observations by CT/MRI [6–9] and from a recent systematic review and meta-analysis which reported a 38% (95% CI, 31–45%) of HCC risk in LR-3 category [18]. However, to properly interpret the results of studies about LI-RADS categorization, it is a key to evaluate if the cohort of patients has been collected prospectively, if there was prior US detection within a surveillance program of the population at risk of developing HCC, and if the final diagnosis has been set by pathology as an optimal gold standard. For instance, in a study of Tanabe et al [7] that suggests that LR-3 observations should be seen as a very low likelihood of HCC development, it is reported that 151 out of 166 LR-3 observations remained stable or decreased in category after a median

**Table 5** MRI features of lesions categorized as LR-3

| | All nodules ($n$ = 74) | HCC ($n$ = 51) | Non-HCC ($n$ = 23)* | $p$ value |
|---|---|---|---|---|
| Size by MRI (median [range], in mm) | 14 [5–22] | 14 [8–22] | 12 [5–20] | *< 0.001* |
| < 10 mm, $n$ (%) | 5 (6.7) | 0 (0) | 5 (21.7) | |
| 10–15 mm, $n$ (%) | 48 (64.9) | 31 (60.8) | 17 (73.9) | |
| 16–20 mm, $n$ (%) | 20 (27.0) | 19 (37.2) | 1 (4.3) | |
| > 20 mm, $n$ (%) | 1 (1.4) | 1 (2) | 0 (0) | |
| T1 weighted imaging, $n$ (%) | | | | |
| Not seen | 18 (24.3) | 10 (19.6) | 8 (34.8) | *0.034* |
| Isointense | 12 (16.2) | 8 (15.7) | 4 (17.4) | |
| Hypointense | 14 (18.9) | 7 (13.7) | 7 (30.4) | |
| Hyperintense | 30 (40.5) | 26 (51.0) | 4 (17.4) | |
| T2-weighted imaging, $n$ (%) | | | | |
| Not seen | 25 (33.8) | 17 (33.3) | 8 (34.8) | 0.15 |
| Isointense | 16 (21.6) | 14 (27.5) | 2 (8.7) | |
| Hypointense | 10 (13.5) | 4 (7.8) | 6 (26.1) | |
| Hyperintense | 23 (31.1) | 16 (31.4) | 7 (30.4) | |
| Arterial phase, $n$ (%) | | | | |
| Not seen | 4 (5.4) | 4 (7.8) | 0 (0) | 0.16 |
| Isointense | 10 (13.5) | 6 (11.7) | 4 (17.4) | |
| Hypointense | 6 (8.1) | 3 (5.9) | 3 (13.0) | |
| Hyperintense | 54 (73) | 38 (74.5) | 16 (69.6) | |
| Portal venous phase, $n$ (%) | | | | |
| Not seen | 14 (18.9) | 9 (17.6) | 5 (21.7) | 0.64 |
| Isointense | 22 (29.7) | 17 (33.3) | 5 (21.7) | |
| Hypointense | 13 (17.6) | 9 (17.7) | 4 (17.4) | |
| Hyperintense | 25 (33.8) | 16 (31.4) | 9 (39.1) | |
| Delayed venous phase, $n$ (%) | | | | |
| Not seen | 16 (21.6) | 11 (21.6) | 5 (21.7) | 0.24 |
| Isointense | 26 (35.1) | 21 (41.2) | 5 (21.7) | |
| Hypointense | 18 (24.3) | 12 (23.5) | 6 (26.1) | |
| Hyperintense | 14 (18.9) | 7 (13.7) | 7 (30.4) | |
| Non-peripheral washout (yes/no), $n$ (%) | 0/74 (0/100) | 0/51 (0/100) | 0/23 (0/100) | 1 |
| Enhancing capsule (yes/no), $n$ (%) | 2/72 (2.7/97.3) | 2/49 (3.9/96.1) | 0/23 (0/100) | 1 |
| Intralesional fat (yes/no), $n$ (%) | 7/67 (9.5/90.5) | 5/46 (9.8/90.2) | 2/21 (8.7/91.3) | 1 |

*This category includes a 14-mm intrahepatic cholangiocarcinoma and a 15-mm colorectal adenocarcinoma metastasis

The variables with $p$ value ≤ 0.005 are set in italics

imaging follow-up of 538 days. However, none of these LR-3 observations was assessed histologically, and the LI-RADS category assignment was based on the retrospective evaluation of the radiological reports.

When we compared the main radiological findings of LR-3 observations between HCC and non-HCC lesions, ancillary features of malignancy as hyperintensity on T2-weighted imaging or presence of intralesional fat [19–21] were not more frequent in LR-3 HCC lesions. Nodule size at MRI became the most relevant parameter associated with HCC diagnosis. In our series, 20 out of 21 LR-3 nodules > 15 mm (95.2%) were finally diagnosed as HCC. Contrarily, none of the LR-3 nodules < 10 mm was finally confirmed as HCC. Based on our results, in our opinion, the cutoff size to stratify LI-RADS categories could be set at 15 mm. This suggestion should be explored by other groups and, if confirmed, will change the current proposal. Keeping the 20 mm cutoff may be appealing because of the policy for liver transplantation indication, but it is worth to recall that patients with very early HCC may benefit from ablation or resection, while never being considered for transplant because of comorbidities or lack of such option in their country.

The high probability that a new nodule detected by US in cirrhotic patients categorized as LR-3 corresponds to an HCC justifies triggering an active diagnostic work-up including biopsy and/or close imaging follow-up if we are intended to diagnose and treat the HCC at a very early stage, when the probability of dissemination is very low [22] and the outcome after resection or ablation is excellent [2, 3].

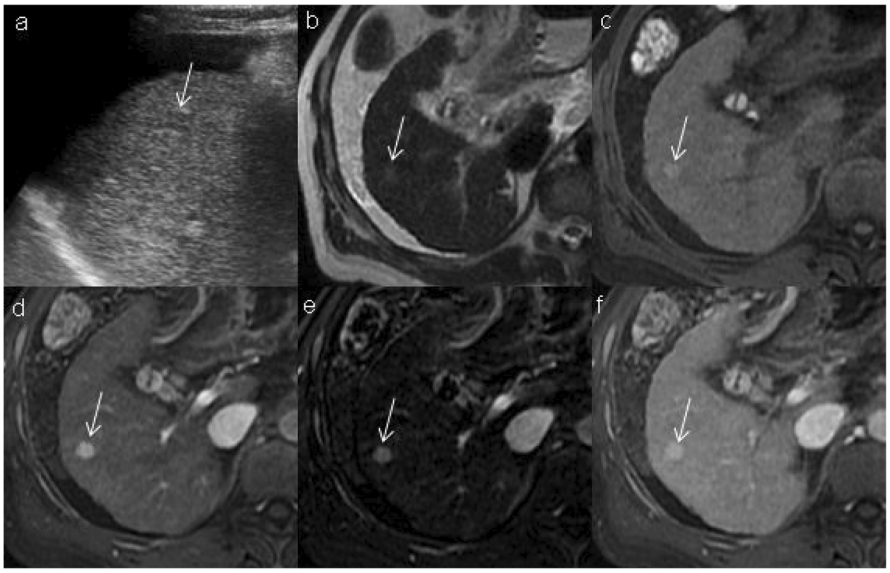


**Fig. 2** Eleven-millimeter US-detected nodule (arrow) in segment V (**a**). The nodule (arrows) is slightly hyperintense on T2-weigthed images (**b**) and hyperintense on T1-weighted images before contrast administration (**c**). It shows arterial phase hyperenhancement (arterial phase and subtraction sequences; **d** and **e**, respectively) but not washout nor pseudocapsule on delayed venous phase (**f**). A LI-RADS 3 category was assigned. Histological analysis after FNB showed that the nodule corresponded to a well-differentiated HCC

Furthermore, this study confirms our previous observation that near one-quarter of nodules categorized as LR-2 are finally diagnosed as HCC (6 out of 26, 23.1%). More interestingly, the median time for HCC diagnosis was 4.5 months, and thus the recommendation of not engaging any additional studies except continuing the routine surveillance every 6 months [10] may not be supported by our results. In our opinion, a 23% risk of HCC may justify an active diagnostic work-up [23], but additional studies including more LR-2 observations in US-detected nodules are needed to support our suggestion.

The major modification implemented in the LI-RADS v2018 was the change of categorization in observations 10–19 mm with arterial phase hyperenhancement and non-peripheral *washout* from LR-4 to LR-5 regardless of appearance on antecedent surveillance US images [11, 24]. In our study, observations categorized as LR-5 as defined in LI-RADS v2018 displayed a sensitivity of 64% (95% CI, 56.8–70.7), figures very similar when EASL criteria [2] were applied in our cohort, and in line with the reported by other authors when these criteria were evaluated [12–14, 25–27]. Very interestingly, with the new update of v2018, there is a significant drop of observations categorized as LR-4 compared with previous studies [5, 18]. Furthermore, 11 out of 12 observations categorized as LR-4 were finally diagnosed as HCC, and when combined all together LR-4 and LR-5 observations, the diagnostic accuracy did not differ significantly and thus questioning the need of distinguishing between both categories in newly detected nodules by screening US.

Our study has limitations: LI-RADS category assignment was done after consensus interpretation by two radiologists, and we have not evaluated the inter-observer agreement. This is relevant since, in real life, LI-RADS categories are assigned by one radiologist, and there is a substantial variation in liver observation reported by both experts and novices when a standardized reporting schema is used [28]. Furthermore, we have not considered ancillary findings in our assessment of LR-3, LR-4, and LR-5 observations. However, as clearly stated in the LI-RADS v2018 proposal, ancillary features are optional and may be used at radiologist discretion, and their use does not allow to upgrade the LI-RADS category to LR-5 [29]. The application of these ancillary findings has been shown useful for increasing the sensitivity but in detriment of worse specificity [30]. In addition, avoiding the use of ancillary findings, we reduce the radiologist-dependent subjectivity and allow translating our results to CT since most of those ancillary findings are only available when using MR, and some of them only when using hepatobiliary agents.

In conclusion, 69% of our newly detected nodules by screening US categorized as LR-3 are HCC, being particularly true in nodules larger than 15 mm. Our data suggest that if LI-RADS is applied, an active diagnostic work-up including biopsy is justified in US-detected LR-3 observations if aimed to treat HCC at a very early stage.

**Supplementary Information** The online version contains supplementary material available at https://doi.org/10.1007/s00330-020-07457-6.

**Acknowledgments** Álvaro Díaz-González: Grant support from the Instituto de Salud Carlos III (CM15/00050) and Ayuda Clínico Junior 2018 from the Asociación Española Contra el Cáncer (AECC).

María Reig: Grant support from Instituto de Salud Carlos III (PI15/00145 and PI18/00358).

Jordi Bruix: Grant support from Instituto de Salud Carlos III (PI14/00962 and PI18/00768), AECC (PI044031), Secretaria

d'Universitats i Recerca del Departament d'Economia i Coneixement (2014 SGR 605), and WCR (AICR) 16-0026.

Alejandro Forner: Grant support from Instituto de Salud Carlos III (PI13/01229 and PI18/00542).

CIBERehd is funded by the Instituto de Salud Carlos III.

**Funding** This study has received funding by Instituto de Salud Carlos III (PI18/00542).

## Compliance with ethical standards

**Guarantor** The scientific guarantor of this publication is Alejandro Forner.

**Conflict of interest** The authors of this manuscript declare relationships with the following companies:

Anna Darnell, Álvaro Díaz-González, and Carmen Ayuso: Speaker fees and travel grants from Bayer.

Jordi Rimola: Speaker fees and travel grants from Bayer. Consultancy fees COR2ED.

Ernest Belmonte: Travel grants from BTG.

Enric Ripoll, Carla Caparroz, and Ramón Vilana: None.

Ángeles García-Criado: Speaker fees from BTG and Terumo.

María Reig: Consultancy from Bayer, BMS, Roche, Ipsen, AstraZeneca, and Lilly. Lecture fees from Bayer, BTG, BMS, Gilead, and Lilly. Research grants from Bayer and Lilly.

Jordi Bruix: Consultancy from Arqule, Bayer, Novartis, BMS, BTG-Biocompatibles, Eisai, Kowa, Terumo, Gilead, Bio-Alliance, Roche, AbbVie, Merck, Sirtex, Ipsen, Astra-Medimmune, Incyte, Quirem, Adaptimmune, and Lilly. Research grants from Bayer and BTG. Educational grants from Bayer and BTG. Lecture fees from Bayer, BTG-Biocompatibles, Eisai, Terumo, Sirtex, and Ipsen.

Alejandro Forner: Speaker fees from Bayer, Gilead, and MSD; consultancy fees from Bayer, AstraZeneca, and Guerbert.

None of those declared company relationships are related to the subject matter of the article.

**Statistics and biometry** No complex statistical methods were necessary for this paper. Noteworthy, the corresponding author of this article (Alejandro Forner) has a degree on Investigation Methodology in Health Science and a Master in Methodology of Investigation in Health Science by the Universidad Autónoma de Barcelona, Spain.

**Informed consent** Written informed consent was waived by the institutional review board.

**Ethical approval** Institutional review board approval was obtained.

**Study subjects or cohorts overlap** Part of the population study was previously reported to validate the non-invasive diagnostic criteria for hepatocellular carcinoma (Forner A et al *Hepatology* 2008; 47:97–104), the limited value of intratumoral fat or peritumoral capsule to increase the diagnostic accuracy of MRI (Rimola J et al *Journal of Hepatology* 2012;56:1317–1323), and the evaluation of the diagnostic accuracy of LI-RADS v2013 (Darnell A et al *Radiology*. 2015;275:698–707). However, the results of the present study and the previous do not overlap and do not contain redundant information. In particular, the latter study in 2015 by Darnell et al included 133 patients and the lesions were evaluated according to LI-RADS v2013. In the present study, we included 129 additional patients, and the LI-RADS assessment was done with v2018.

**Methodology**
- Retrospective analysis of a prospective protocol
- Diagnostic or prognostic study
- Performed at one institution

## References

1. Alazawi W, Cunningham M, Dearden J, Foster GR (2010) Systematic review: outcome of compensated cirrhosis due to chronic hepatitis C infection. Aliment Pharmacol Ther 32:344–355. APT4370. https://doi.org/10.1111/j.1365-2036.2010.04370.x
2. Galle PR, Forner A, Llovet JM et al (2018) EASL clinical practice guidelines: management of hepatocellular carcinoma. J Hepatol 69: 182–236. https://doi.org/10.1016/j.jhep.2018.03.019
3. Heimbach JK, Kulik LM, Finn RS et al (2018) AASLD guidelines for the treatment of hepatocellular carcinoma. Hepatology 67:358–380. https://doi.org/10.1002/hep.29086
4. Elsayes KM, Kielar AZ, Agrons MM et al (2017) Liver Imaging Reporting and Data System: an expert consensus statement. J Hepatocell Carcinoma 4:29–39. https://doi.org/10.2147/JHC.S125396
5. Darnell A, Forner A, Rimola J et al (2015) Liver Imaging Reporting and Data System with MR imaging: evaluation in nodules 20 mm or smaller detected in cirrhosis at screening US. Radiology 275: 698–707. https://doi.org/10.1148/radiol.15141132
6. Choi J-Y, Cho HC, Sun M et al (2013) Indeterminate observations (liver imaging reporting and data system category 3) on MRI in the cirrhotic liver: fate and clinical implications. AJR Am J Roentgenol 201:993–1001. https://doi.org/10.2214/AJR.12.10007
7. Tanabe M, Kanki A, Wolfson T et al (2016) Imaging Outcomes of Liver Imaging Reporting and Data System version 2014 category 2, 3, and 4 observations detected at CT and MR imaging. Radiology 281:129–139. https://doi.org/10.1148/radiol.2016152173
8. Liu W, Qin J, Guo R et al (2018) Accuracy of the diagnostic evaluation of hepatocellular carcinoma with LI-RADS. Acta Radiol 59: 140–146. https://doi.org/10.1177/0284185117716700
9. Kierans AS, Makkar J, Guniganti P et al (2018) Validation of Liver Imaging Reporting and Data System 2017 (LI-RADS) criteria for imaging diagnosis of hepatocellular carcinoma. J Magn Reson Imaging. https://doi.org/10.1002/jmri.26329
10. American College of Radiology. Liver Imaging Reporting and Data System version 2018. Accessed March 12 2020, from https://www.acr.org/-/media/ACR/Files/RADS/LI-RADS/LI-RADS-2018-Core.pdf?la=en
11. Chernyak V, Fowler KJ, Kamaya A et al (2018) Liver Imaging Reporting and Data System (LI-RADS) version 2018: imaging of hepatocellular carcinoma in at-risk patients. Radiology 289:816–830. https://doi.org/10.1148/radiol.2018181494
12. Forner A, Vilana R, Ayuso C et al (2008) Diagnosis of hepatic nodules 20 mm or smaller in cirrhosis: prospective validation of the noninvasive diagnostic criteria for hepatocellular carcinoma. Hepatology 47:97–104. https://doi.org/10.1002/hep.21966
13. Khalili KT, Kim TK, Jang HJ et al (2011) Optimization of imaging diagnosis of 1-2 cm hepatocellular carcinoma: an analysis of diagnostic performance and resource utilization. J Hepatol 54:723–728. https://doi.org/10.1016/j.jhep.2010.07.025
14. Sangiovanni A, Manini MA, Iavarone M et al (2010) The diagnostic and economic impact of contrast imaging technique in the diagnosis of small hepatocellular carcinoma in cirrhosis. Gut 59:638–644. https://doi.org/10.1136/gut.2009.187286
15. International Consensus Group for Hepatocellular NeoplasiaThe International Consensus Group for Hepatocellular Neoplasia (2009) Pathologic diagnosis of early hepatocellular carcinoma: a

report of the international consensus group for hepatocellular neoplasia. Hepatology 49:658–664. https://doi.org/10.1002/hep.22709
16. Abd Alkhalik Basha M, Abd El Aziz El Sammak D, El Sammak AA (2017) Diagnostic efficacy of the Liver Imaging-Reporting and Data System (LI-RADS) with CT imaging in categorising small nodules (10–20 mm) detected in the cirrhotic liver at screening ultrasound. Clin Radiol 72:901.e1–901.e11. https://doi.org/10.1016/j.crad.2017.05.019
17. Basha MAA, AlAzzazy MZ, Ahmed AF et al (2018) Does a combined CT and MRI protocol enhance the diagnostic efficacy of LI-RADS in the categorization of hepatic observations? A prospective comparative study. Eur Radiol 28:2592–2603. https://doi.org/10.1007/s00330-017-5232-y
18. van der Pol CB, Lim CS, Sirlin CB et al (2019) Accuracy of the Liver Imaging Reporting and Data System in computed tomography and magnetic resonance image analysis of hepatocellular carcinoma or overall malignancy—a systematic review. Gastroenterology 156:976–986. https://doi.org/10.1053/j.gastro.2018.11.020
19. Willatt JM, Hussain HK, Adusumilli S, Marrero JA (2008) MR imaging of hepatocellular carcinoma in the cirrhotic liver: challenges and controversies. Radiology 247:311–330
20. Khan AS, Hussain HK, Johnson TD et al (2010) Value of delayed hypointensity and delayed enhancing rim in magnetic resonance imaging diagnosis of small hepatocellular carcinoma in the cirrhotic liver. J Magn Reson Imaging 32:360–366. https://doi.org/10.1002/jmri.22271
21. Kim TK, Lee KH, Jang HJ et al (2011) Analysis of gadobenate dimeglumine-enhanced MR findings for characterizing small (1-2-cm) hepatic nodules in patients at high risk for hepatocellular carcinoma. Radiology 259:730–738. https://doi.org/10.1148/radiol.11101549
22. Roskams T, Kojiro M (2010) Pathology of early hepatocellular carcinoma: conventional and molecular diagnosis. Semin Liver Dis 30:17–25. https://doi.org/10.1055/s-0030-1247129
23. Bruix J, Ayuso C (2019) Diagnosis of hepatic nodules in patients at risk for hepatocellular carcinoma: LIRADS probability vs certainty. Gastroenterology 156:860–862. https://doi.org/10.1053/j.gastro.2019.02.008
24. Kielar AZ, Chernyak V, Bashir MR et al (2019) An update for LI-RADS: version 2018. Why so soon after version 2017? J Magn Reson Imaging 50:1990–1991. https://doi.org/10.1002/jmri.26715
25. Leoni S, Piscaglia F, Golfieri R et al (2010) The impact of vascular and nonvascular findings on the noninvasive diagnosis of small hepatocellular carcinoma based on the EASL and AASLD criteria. Am J Gastroenterol 105:599–609. https://doi.org/10.1038/ajg.2009.654
26. Kim SE, Lee HC, Shim JH et al (2011) Noninvasive diagnostic criteria for hepatocellular carcinoma in hepatic masses larger than 2 cm in a hepatitis B virus-endemic area. Liver Int 31:1468–1476. https://doi.org/10.1111/j.1478-3231.2011.02529.x
27. Erkan B, Meier J, Clark TJ et al (2019) Non-invasive diagnostic criteria of hepatocellular carcinoma: comparison of diagnostic accuracy of updated LI-RADS with clinical practice guidelines of OPTN-UNOS, AASLD, NCCN, EASL-EORTC, and KLSCG-NCC. PLoS One 14:e0226291. https://doi.org/10.1371/journal.pone.0226291
28. Davenport MS, Khalatbari S, Liu PSC et al (2014) Repeatability of diagnostic features and scoring systems for hepatocellular carcinoma by using MR imaging. Radiology 272:132–142. https://doi.org/10.1148/radiol.14131963
29. Cerny M, Chernyak V, Olivié D et al (2018) LI-RADS version 2018 ancillary features at MRI. Radiographics 38:1973–2001. https://doi.org/10.1148/rg.2018180052
30. Kang JH, Choi SH, Byun JH et al (2020) Ancillary features in the Liver Imaging Reporting and Data System: how to improve diagnosis of hepatocellular carcinoma ≤ 3 cm on magnetic resonance imaging. Eur Radiol. https://doi.org/10.1007/s00330-019-06645-3

**Publisher's note** Springer Nature remains neutral with regard to jurisdictional claims in published maps and institutional affiliations.